Solar Energy Materials & Solar Cells 275 (2024) 113036

Contents lists available at ScienceDirect

Solar Energy Materials and Solar Cells

journal homepage: www.elsevier.com/locate/solmat

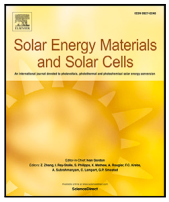

Light induced degradation of CIGS solar cells

T.S. Vaas [a,b,*], B.E. Pieters [a], D. Roosen-Melsen [c], M. van den Nieuwenhof [c], A. Kingma [c], M. Theelen [c], C. Zahren [a], A. Gerber [a], U. Rau [a,b]

[a] IMD3-Photovoltaics, Forschungszentrum Jülich GmbH, Wilhelm-Johnen Straße, Jülich, 52425, North Rhine-Westphalia, Germany
[b] Jülich Aachen Research Alliance (JARA-Energy) and Faculty of Electrical Engineering and Information Technology, RWTH Aachen University, Schinkelstraße 2, Aachen, 52062, North Rhine-Westphalia, Germany
[c] TNO partner in Solliance, High Tech Campus 21, Eindhoven, 5656 AE, Noord-Brabant, The Netherlands

ARTICLE INFO

Keywords:
CIGS
Degradation
LID
Performance stability

ABSTRACT

Considering warranted lifetimes of PV modules of typically 20-30 years, the performance stability of PV modules is one of the most crucial factors regarding power generation and yield. Long term outdoor performance studies depict realistic operation conditions best, but the correlated nature of e.g. irradiance and temperature impedes the physical interpretation. The possibility to control and tune the conditions in laboratory experiments enables to decompose effects, that are typically overlayed in outdoor experiments. This way, laboratory are crucial to interpret the results obtained in outdoor degradation studies. One driving force of degradation of CIGS modules is light exposure. In literature the focus of light induced degradation (LID) of CIGS modules and solar cells is on metastable changes analyzed on time scales ranging from minutes to hours. In this work we expose industrially produced encapsulated CIGS solar cells for more than 1000 h to light with varied intensity under varied temperature conditions. Such, we aim to study temperature and light intensity dependencies of the observed performance changes. Furthermore, we study the influence of applied bias by comparing LID at short and open circuit. We demonstrate that LID under short circuit conditions leads to V_{OC} degradation, while being temperature assisted and not dependent on the irradiance intensity. CIGS solar cells kept at open circuit conditions appear to be stable under illumination. Exploiting the one diode model, we further connect the observed temperature assisted performance loss to enhanced recombination with lower ideality factor, in comparison to the dominant recombination process before degradation.

1. Introduction

Copper Indium Gallium Diselenide Cu(In,Ga)Se_2 (CIGS) solar cells achieved a current record efficiency of 23.6% [1] and have therefore shown to be competitive to the more established wafer based technologies. Especially due to the feasibility of CIGS solar cells in flexible and light weight photovoltaic (PV) applications, the technology possesses a potential growth in the integrated PV market, e.g. in the vehicle integrated PV (VIPV) and building integrated PV (BIPV) market.

For all PV applications the durability and performance stability of devices is a crucial factor. For conventional glass-glass CIGS modules the performance degradation has been studied in great detail as comprehensively summarized in the two review articles from [2] respectively [3]. Long term studies on the performance under outdoor conditions, such as those performed in Refs. Schweiger et al. [4], Makrides et al. [5], are ultimately the best way to evaluate the stability of CIGS modules as the conditions are closest to realistic operation conditions. Under outdoor conditions conventional CIGS modules are shown to experience a performance drop in the beginning of operation (acclimatization) [4] overlayed with seasonal variations and a linear degradation [4,5]. While the research on outdoor degradation shows a clear trend, the exact causes for the observed acclimatization, seasonality and degradation are hard to infer from such measured time series. Under outdoor conditions various factors like temperature, irradiance (long and short wavelength visible as well as UV), humidity, wind as well as soiling, may influence the modules performance. Furthermore, the conditions are highly correlated, e.g. PV modules heat up under illumination, leading to a clear correlation of irradiance and module temperature.

Laboratory experiments are more suited to study the isolated effects from the various influences by an accurate control of the degradation conditions. Hence, laboratory experiments can be used to elaborate on the insights on degradation of CIGS modules gained in outdoor studies. Another advantage of laboratory experiments is the time scale. Where outdoor studies have to be performed over years to make meaningful

* Corresponding author at: IMD3-Photovoltaics, Forschungszentrum Jülich GmbH, Wilhelm-Johnen Straße, Jülich, 52425, North Rhine-Westphalia, Germany.
E-mail address: t.vaas@fz-juelich.de (T.S. Vaas).

https://doi.org/10.1016/j.solmat.2024.113036
Received 13 May 2024; Received in revised form 1 July 2024; Accepted 4 July 2024
Available online 14 July 2024
0927-0248/© 2024 The Author(s). Published by Elsevier B.V. This is an open access article under the CC BY-NC-ND license (http://creativecommons.org/licenses/by-nc-nd/4.0/).

statements about the stability, such laboratory experiments can provide more extreme conditions (e.g. high irradiance, high humidity, high temperature) which allow for much shorter time spans.

One aspect of outdoor degradation is the influence of illumination on the CIGS module performance, i.e. light induced degradation (LID). In literature, effects of illumination on the performance of CIGS solar cells is mainly focused on metastable performance changes [6–10] evaluating performance changes over short time periods, i.e. over minutes to hours. Walkons et al. describe a light soaking experiment of up to ≈135 h on differently produced CIGS solar cells[1] [11]. Cells from two different batches produced with different alkali treatments were subject to the study. Each cell type was exposed to 1000 W/m^2 of AM1.5 g light at different temperatures between 50 and 85 °C and short circuit (SC) as well as open circuit (OC) conditions. Walkons et al. observe an increase in V_{OC} upon light soaking under OC and a decrease under SC conditions. An increased degradation temperature seems to enhance the observed impact on V_{OC}. Furthermore, RbF Post deposition treatment (PDT) is shown to lead to more stable performance under illumination [11].

In this work we systematically study the dependency of light induced degradation (LID) of CIGS devices on the light intensity, temperature and bias condition on a time scale of more than 1000 h. We expose a set of industrially produced and encapsulated CIGS solar cells to light under different illumination intensities, temperature and bias conditions. To gain insights on the interplay of light and temperature we expose the solar cells to three different temperatures between 25 and 70 °C and four light intensities between 0 and 1000 W/m^2. All combinations of temperature and light intensity are studied, keeping one set of cells at SC and another set of cells at OC. With frequent in situ JV measurements as well as with a detailed ex situ characterization before and after ≈1170 h of light exposure we show, that the conditions during light exposure strongly influence the observed performance changes.

Before we discuss our experiments in detail we first give a small overview of laboratory (accelerated) degradation testing and the theory behind the observed degradation and the metastable changes in Section 2. In Section 3 we comprehensively explain the measurement procedure, describe the sample preparation and discuss the used setups. Section 4 displays the main results structured in the solar cells performance before LID, the in situ observed changes and the ex situ verified comparison of the solar cells performance before and after LID. In Section 5 we derive deeper insights on the observed changes employing the one-diode model. Finally, in Section 6 the major results are summarized and an outlook on future work is given.

2. CIGS degradation, accelerated testing and metastabilities

Long term degradation studies, such as those in Refs. Schweiger et al. [4] and Makrides et al. [5], are both tedious and expensive. Ideally, the duration of such long term degradation studies would be oriented towards the module lifetime itself, however, with a warranted lifetime of PV modules of typically 20–30 years this is unfeasible. Consequently, such studies are limited to one or a few years, which may be enough to study the mayor effects in long term degradation. Arguably, the economic lifetime of PV modules is likely much shorter [12]. However, one of the reasons that the economic lifetime of PV modules is much shorter is the technological advances over time [12], which in turn implies a risk that the outcome of a long term degradation experiment is outdated before it is completed.

Research on degradation of CIGS modules (and PV modules in general) tends to focus on accelerated aging tests, evaluating the susceptibility of the modules to common causes of degradation in operation. Damp Heat (DH) testing quantifies their susceptibility to humidity and temperature [13–20]. In general a performance loss is observed under DH, which is associated with a decrease in open circuit voltage (V_{OC}), short circuit current (I_{SC}), fill factor (FF), and shunt resistance (R_{sh}), as well as an increase in series resistance (R_S). The performance loss ratios appear to be highly dependent on the packaging material, encapsulant as well as the solar cell stack itself (e.g. TCO and buffer layer). Suitable packaging and encapsulation materials can prevent high performance loss ratios due to humidity ingress leading to an enhanced series resistance, i.e. TCO [13–17] respectively molybdenum back contact [18–20] degradation. Furthermore, enhanced shunting due to DH treatment is observed [16,17].

Potential induced degradation (PID) accelerated aging tests on CIGS modules quantify the susceptibility of PV modules to high system voltages common in medium to large PV systems. In literature several studies quantify the performance loss due to PID [21–28]. As for DH treatments the performance loss ratios due to PID are highly dependent on the design and production process of the CIGS module, where a performance drop to close to 0% as well as nearly no performance drop is observed after 50 h of PID for differently produced devices Fjällström et al.. Here, high performance loss rates are associated with a large drop in V_{MPP} associated with a large V_{OC} degradation. Further studies on PID find increased bulk and interface defect concentrations [22], a decreased bulk doping concentration [23] as well as an increase in the series resistance due to TCO degradation [25,26]. Furthermore, PID appears to be dependent on the applied bias condition of the PV module, where faster degradation rates are found for short circuited modules w.r.t open circuited modules [27]. Fjällström et al. further observe non-permanent PID with restored electrical performance close to initial performance after storage in darkness or reversing the electric field that led to the PID [28].

The observed reversibility of PID introduces another complexity. Observed performance changes of CIGS solar cells and modules have to be considered in the context of metastabilities. The metastable nature of CIGS solar cells has already been observed decades ago [6]. Phenomenological it has been found, that CIGS solar cells and thin films exhibit persistent photoconductivity (PPC) due to illumination [29]. Furthermore, under white light illumination (light soaking) a gain in V_{OC}, FF and capacitance has been observed [6–10], where the gain in capacitance as well as in conductivity is attributed to red light illumination (absorption in the CIGS absorber) [10,30,31] and the gain in FF attributed to blue light illumination (absorption in the CdS buffer layer) [32]. Under forward bias CIGS solar cells are shown to exhibit a gain in V_{OC} as well as in capacitance [6–8,33–35].

Recent studies on metastabilities in CIGS solar cells have shown, that the amplitude of observed metastabilities is dependent on the production process [11,36,37]. Repins et al. examined CIGS metastabilities due to light soaking on devices produced with different buffer layers. The efficiency of the differently produced CIGS solar cells is found to be anti-correlated with the amplitude of metastable V_{OC} changes due to light exposure, where high-efficient solar cells exhibit a less metastable nature [36]. Walkons et al. showed, that, while temperature assisted (65 °C) light soaking at open circuit has a beneficial effect on V_{OC}, temperature assisted light soaking at short circuit conditions has a negative impact on the performance of different CIGS devices [11].

The most common theory in literature to explain the metastable behavior of CIGS solar cells is based on a selenium copper divacancy defect complex ($V_{Se} - V_{Cu}$) in the CIGS absorber first proposed by Lany and Zunger [38]. According to Lany and Zunger the $V_{Se} - V_{Cu}$ defect complex has two configurations, that act as shallow donor and shallow acceptor respectively. Which configuration of the defect complex is dominant thereby depends on the position of the Fermi-level within the bandgap. With a Fermi-level close to the valence band (as in typically p-type CIGS absorbers) the shallow donor configuration is dominant, although the metastable equilibrium of the defect configuration may be shifted by (photo-generated) free electrons. While the presence of such a metastable defect configuration seems to be consistent with

[1] Unfortunately it is unclear whether the used samples are encapsulated or not.

literature it has been shown, that this explanation alone is not sufficient to explain the observed magnitude and timescale of observed metastabilities [39–41].

The high attention in literature on studying DH, PID and metastabilities of CIGS devices indicates that it is a challenging task to gain more insight into the underlying mechanisms. There are several links that copper-, alkali- and in general ion-migration into the device seems to play a crucial role regarding degradation [16,17,21–26] and metastable changes [42–44]. The crucial role of alkali elements is underlined by the recent improvements in efficiency achieved by incorporating alkali-fluoride (i.e. RbF) in post deposition treatments (PDT) [45,46], i.e. leading to a substitution of sodium with heavier and less mobile rubidium atoms. Beside the increased efficiency, RbF PDT seems to reduce the amplitude of the metastable behavior of CIGS solar cells under light exposure [11].

The analysis of ion migration and changed concentrations of for example sodium or copper due to DH, PID, bias or light exposure gains valuable insights on how the stoichiometry in CIGS solar cells affects its performance. However, the influence of e.g. increased sodium content on the band structure or on shallow and deep defect concentrations are not fully understood. Furthermore, a stoichiometric analysis always reflects only a small share of the solar cell not being able to track lateral variations. Because of the variety and complexity of the reactions during the production of CIGS thin films, the low comparability of different cells from different production lines used in different studies impedes the interpretation.

3. Experimental

In total 24 CIGS solar cells are exposed to light induced Degradation (LID). During the LID for 1170 h, 12 cells are kept in short circuit (SC) and 12 cells are kept in open circuit (OC) conditions. Both sets of 12 samples are degraded under 12 different combinations of 3 temperatures ($T_1 = 25\ °C, T_2 = 50\ °C, T_3 = 70\ °C$) and 4 irradiation intensities ($G_0 = 0.0\%$, $G_1 = 13.5\%$, $G_2 = 47.3\%$ and $G_3 = 100.0\%$ of one sun equivalent irradiation).[2]

3.1. Sample preparation

The used samples are cut from two industrial produced flexible $308 \times 44\ mm^2$ CIGS solar cells from MiaSolé that were commercially acquired [47]. The solar cells are produced on a stainless steel substrate used as back contact and the front contact is established using MiaSolé's Ultrawire interconnect technology. From each solar cell we cut 16 similar solar cells with a width of $w_{cell} = 44.0$ mm and a length of $l_{cell} \approx 12.0$ mm. Each solar cell is then contacted with aluminium busbars using a commercial isotropic conductive adhesive and encapsulated by vacuum lamination using a standard layer stack comprising all commercially available flexible frontsheet, flexible backsheet and polyolefin based encapsulants. OMEGA 5SC-TT-K-36-36 thermocouples are placed at the center of the back contact of each cell and encapsulated within.

In total 32 CIGS solar cells were prepared. All 32 cells were characterized using EL and PL imaging as well as with an JV characteristic at standard test conditions (STC, $T = T_1 = 25\ °C$ and $G = G_3$). Afterwards we selected 24 of the 32 cells for the light induced Degradation (LID) experiments aiming to have the most comparable performance throughout the used solar cells. As described the 32 cells are cut from two industrial produced cells. Since during the LID we keep 12 cells in SC and 12 cells in OC, we chose for each condition to use 12 cells, which are cut from the same solar cell. Therefore, we selected 12 out of 16 cells for both conditions.[3] We first excluded solar cells with visible defects in the EL respectively PL images. Furthermore, we chose the 12 samples with the most similar fill factor (FF) of around 73% at standard test conditions (STC).

3.2. Ex situ measurements

After the sample selection we installed the samples in the sample holder, consisting of a copper block (for tempering with a refrigerated/heated bath circulator) and an anodized aluminium block (for holding the ND filters and reducing stray lights). The solar cells are fixed in between the two blocks and soldered to four pin connectors to ensure a steady and low external series resistance during all electrical measurements. Afterwards the solar cells are kept in dark storage for one week till the characterization before the LID.

Directly before and after the LID as well as two weeks after the LID the CIGS solar cells are characterized with a steady state WACOM WXS-140S-Super sun simulator with class A accuracy of the AM1.5G solar spectrum. The JV characteristic of every cell is measured at 12 different conditions (at G_0, G_1, G_2 and G_3 as well as T_1, T_2 and T_3). Thereby, we start at T_1 and measure the JV characteristics at G_0, G_1, G_2, G_3 and again at G_0 followed by measurements at T_2 and T_3 in the same order of irradiation levels. In between the measurements at different temperatures the cells are tempered using a climate chamber.

After the JV characterization, the cells are further characterized with EL and PL images. To this end we use a Princeton instruments Nirvana 640 Indium Gallium Arsenide (InGaAs) camera. The camera is equipped with a 1050 nm band-pass filter with a full width half maximum of 30 nm to block the 808 nm laser bias illumination for the PL experiments. The integration time is set to 100 ms and for both EL and PL, a background image is subtracted. The electrical bias of 0.75 V during the EL experiments is provided by a Keithley 238 high current source measurement unit (SMU). To allow for the sample to reach steady state conditions, the image acquisition starts ≈25 s after the solar cell is biased.

3.3. Light induced degradation set-up and in situ measurements

To ensure constant degradation temperatures the sample holders are thermally decoupled from the set-up and the temperature of the refrigerated/heated bath circulators as well as the room temperature are tracked with PT100 temperature sensors. As light source we use a metal halide lamp HMI 4000 W/DXS - Osram 6000 K with a long pass filter of 390 nm that blocks ultraviolet (UV) light. The set-up is shielded from external light sources and the irradiation level is tracked with a silicon photodiode in the middle of the illuminated area. The homogeneity of the irradiation is verified at the positions of the cells with two reference cells (PRC Krochmann GmbH PRC911214/1 and PRC911214/2 with a BG17 filter of a size by 2 cm × 2 cm) before and directly after the LID to deviations below ±3.3%. We observe an increased intensity as well as a red shift over the course of the 1170 h of LID. The total intensity measured by PRC1 increased by +0.7% and the filtered short wavelength intensity measured by PRC2 decreased by −4.7%.

For the complete duration of 1170 h of the LID the samples are not moved to a different set-up and only characterized in situ. Each solar cell is characterized every 30 min with an JV characteristic at the specific conditions the cell is degraded at. In between the JV measurements the samples are kept under the respective OC and SC conditions, where the connected cable ends are either open or connected to each other by a relay control. This means that the cable resistance determines the operating point for the cells kept in SC. The

[2] To create an irradiance level of 13.5 respectively 47.3% we use neutral density (ND) filters. The spectral transmittance of the used ND filters can be found in the Appendix in Fig. 10.

[3] Note, that both used solar cells are from the same production line ensuring a comparability of the results obtained at OC and SC.

Table 1
Standard solar cell parameters of the CIGS solar cells at STC before LID.

V_{OC}	739.5	± 2.4	mV	V_{MPP}	596.7	± 2.5	mV
J_{SC}	33.8	± 0.8	mA/cm^2	J_{MPP}	30.6	± 0.8	mA/cm^2
FF	73.0	± 0.6	%	$\eta_{corrected}$	17.83	± 0.14	%

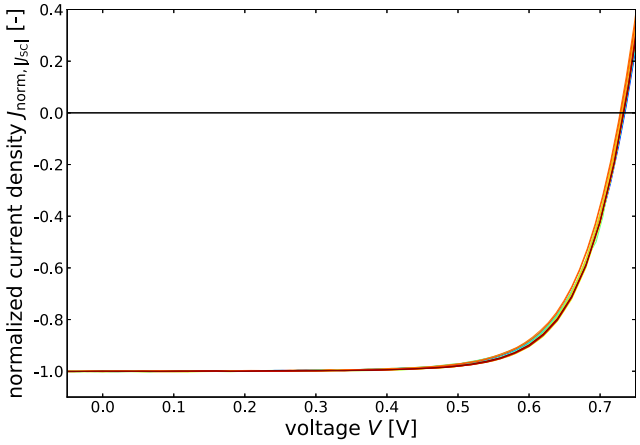

Fig. 1. JV characteristics of the 24 used CIGS solar cells at STC. The current density is normalized to the individual short circuit current densities J_{SC}.

temperatures of the cells are tracked for every JV measurement with the encapsulated thermocouples. Due to the laboratory environment and the constant light source, the humidity can be considered very low during the LID. Furthermore, the samples are encapsulated ensuring no effects originating from water ingress.

4. Results

4.1. Performance before LID

Before the LID all 24 cells show a good and very similar performance. Table 1 summarizes the mean and standard deviation of the standard solar cell parameters (SSPs), i.e. V_{OC}, J_{SC}, V_{MPP} and J_{MPP}, measured under STC for the 24 used solar cells. For the open circuit voltage (V_{OC}) at STC we find a mean of 739.5 mV and a low standard deviation of 2.4 mV among the 24 cells. The maximum power point voltage (V_{MPP}) at STC shows a comparable scatter ($\sigma_{V_{OC}} = 2.5$ mV) with a mean of 596.7 mV. A larger scatter is observed for the short circuit and maximum power point current densities (J_{SC} and J_{MPP}) at STC with a mean of 33.8 mA/cm^2 respectively 30.6 mA/cm^2. This we attribute to the variations in the sample preparation described in Section 3.1. We assume constant dimensions given in Section 3.1, but deviations in the cell length and therefore in the cell area occur due to the cutting process. We find a standard deviation of 2.4% and 2.6% in J_{SC} and J_{MPP} respectively. Regarding the FF at STC we find very low scatter with a mean of 73.0% and a standard deviation of 0.6%. To compare the efficiency without the dominating effect of varying J_{SC} and J_{MPP} we correct the current density values of every individual STC measurement with the ratio of mean to measured J_{SC}. This way, we find an efficiency of $\eta_{corrected} = 17.83 \pm 0.14\%$ for the 24 solar cells.

To further demonstrate the comparability in performance of the 24 solar cells Fig. 1 shows the JV characteristics of all 24 cells at STC conditions. Note that the current densities are normalized with J_{SC} to remove the effect of varying cell area. As described in Section 3.2 all 24 cells are characterized at the sun simulator at 11 further conditions. Regarding the scatter within the batch of used solar cells for the performance at the other G and T conditions we find similar relative standard deviations (not shown) as for the case of the comparison shown for STC.

4.2. Degradation of the SSPs (in situ)

In situ the CIGS solar cells are characterized with an JV measurement every 30 min at the specific conditions the cell is degraded at like described in Section 3.3. First of all we observe no clear trend of decrease or increase in J_{SC} respectively J_{MPP} for all monitored cells.[4] Variations in J_{SC} respectively J_{MPP} occur mainly due to variations in the intensity of the light source and show a similar pattern for all monitored cells (not shown).

The development of the open circuit voltage V_{OC} and maximum power point voltage V_{MPP} exhibit a systematic evolution over time, depending on the bias conditions. We therefore concentrate on V_{OC} hereinafter. Fig. 2(a) shows ΔV_{OC}, the difference between the in situ measured V_{OC} and the first respective measured V_{OC} after the start of LID[5] for the nine cells degraded at open circuit conditions and at irradiation intensities $G > 0$. We observe a clear trend of increasing V_{OC} for the first few hours of LID at open circuit conditions for all 9 cells. For the 3 cells degraded at $T_1 = 25$ °C (yellow) this increase is observed over the whole duration of LID of about 1170 h. For the 3 cells degraded at $T_2 = 50$ °C (red) the increase in V_{OC} saturates after approximately 400 h of degradation. For the 3 cells degraded at $T_3 = 70$ °C (brown) the steep increase in V_{OC} within the first 40 h of LID is followed by a less gradual decrease of V_{OC}. Furthermore, after approximately 78 h of LID we observe an increased V_{OC} for around 35 h, this coincides and is explained with a failure of the $T_3 = 70$ °C water cooling/heating system and resulting slightly lower cell temperatures ($\Delta T = 4$–8K depending on the sample). Comparing the development of ΔV_{OC} of cells degraded at the same degradation temperature and different irradiation intensities we observe a change in amplitude of the effects and trends described. Cells degraded at higher irradiation intensities show higher absolute changes in V_{OC}.

Fig. 2(b) shows the development of ΔV_{OC} for the nine cells degraded at short circuit conditions at irradiation intensities $G > 0$. Contrarily to the case of the samples degraded at OC we do not observe an increase in V_{OC} in the first few hours of LID. For the 3 cells degraded at $T_1 = 25$ °C (yellow) we observe a slow decrease of V_{OC} with a saturation towards the end of the 1170 h of LID. The V_{OC} of the 3 cells degraded at $T_2 = 50$ °C (red) is rather stable during LID, with a slight decrease in V_{OC} at the start of LID. The biggest change in V_{OC} is observed for the 3 samples degraded at $T_3 = 70$ °C (brown) at short circuit conditions, where ΔV_{OC} appears to be stable for the first few hours of LID followed by a steady decrease down to −40 mV ($G = G_1$), to −45 mV ($G = G_3$) respectively −60 mV ($G = G_2$).[6] Furthermore, for some samples we observe a sharp increase respectively a sharp decrease of varying amplitudes, f.e. in the case of the sample degraded at open circuit at $T = T_1$ and $G = G_1$ (yellow triangles in Fig. 2(a)) after approximately 300 h of LID.

4.3. Degradation of the SSPs (ex situ)

As described in Section 3.2 all CIGS solar cells are characterized with JV characteristics at 12 conditions as well as with EL and PL images directly before (pre LID), directly after (after LID) and 2 weeks

[4] Note that 6 cells (SC and OC at 3 different degradation temperatures) are not illuminated and therefore the SSPs cannot be analyzed in situ.

[5] Note that we always compare V_{OC} to the first measurement of the respective cell. Since the cells are measured after each other in an interval of ≈1 min the first respective measurement takes place in between 0 min < t < 24 min after the start of LID. The order of measurements is oriented on the degradation temperature, where the cells degraded at $T_3 = 70$ °C are measured first, followed by the cells degraded at $T_2 = 50$ °C and the cells degraded at $T_1 = 25$ °C.

[6] Note that after 78 h of LID we also observe an increased V_{OC} for around 35 h due to failure of the $T_3 = 70$ °C water cooling/heating system and resulting slightly lower cell temperatures ($\Delta T = 4 - 8$K depending on the sample).

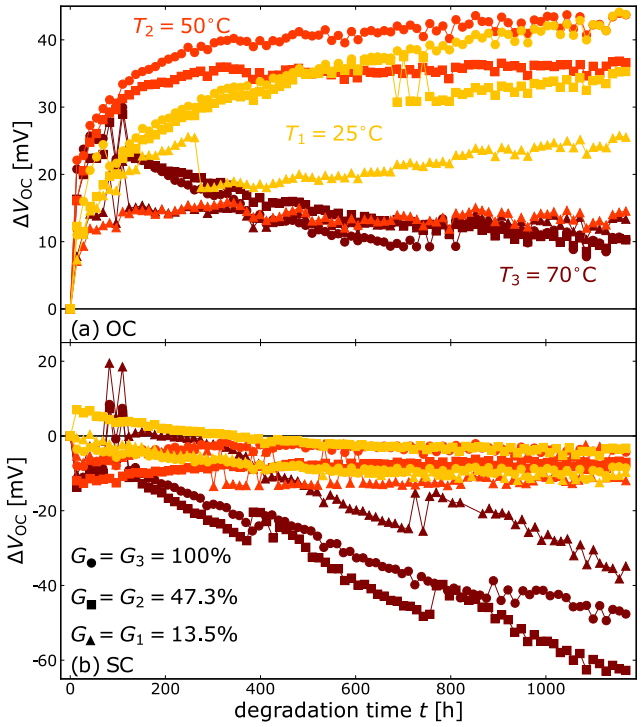

Fig. 2. Absolute change in open circuit voltage ΔV_{OC} due to LID at (a) open circuit and (b) short circuit conditions. The color indicates the degradation temperatures, i.e. yellow corresponds to $T = T_1 = 25$ °C, red to $T = T_2 = 50$ °C and brown to $T = T_3 = 70$ °C. With the markers we differ for the irradiation levels of $G = G_1 = 13.5\%$ (triangles), $G = G_2 = 47.3\%$ (squares) and $G = G_3 = 100\%$ (circles) during degradation.

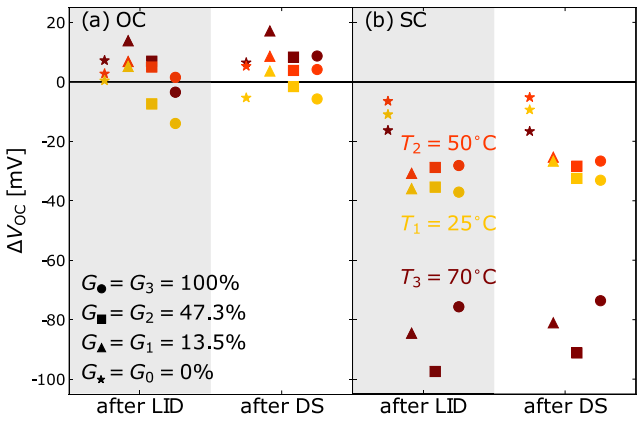

Fig. 3. Absolute change in open circuit voltage ΔV_{OC} at STC due to LID at (a) open circuit and (b) short circuit conditions. The color indicates the degradation temperatures, i.e. yellow corresponds to $T = T_1 = 25$ °C, red to $T = T_2 = 50$ °C and brown to $T = T_3 = 70$ °C. With the markers we differ for the irradiation levels of $G = G_0 = 0\%$ (stars), $G = G_1 = 13.5\%$ (triangles), $G = G_2 = 47.3\%$ (squares) and $G = G_3 = 100\%$ (circles) during degradation.

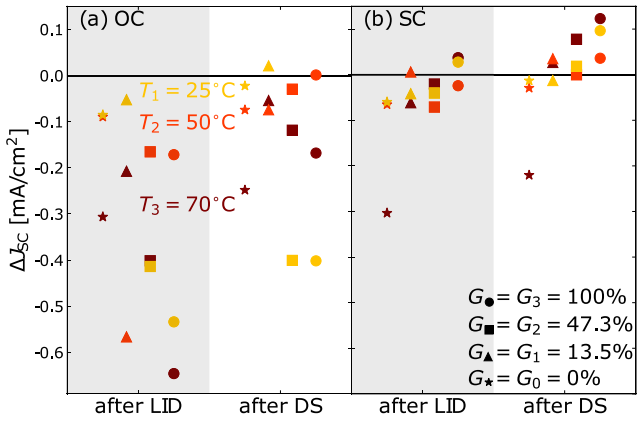

Fig. 4. Absolute change in short circuit current density ΔJ_{SC} at STC due to LID at (a) open circuit and (b) short circuit conditions. To differ between all degradation conditions we use the same color- and marker scheme used before in Figs. 2 and 3.

after the LID, where the cells are kept in dark (after dark storage, DS). Fig. 3(a) shows the change in V_{OC} at STC due to LID at open circuit conditions. All cells degraded at open circuit conditions show a low absolute change in V_{OC} after LID between ±15 mV. Thereby, we observe a tendency for a positive ΔV_{OC} with increasing degradation temperatures. ΔV_{OC} is positive for seven out of 8 samples degraded at $T_2 = 50$ °C (red) or $T_3 = 70$ °C (brown), while ΔV_{OC} is negative for two out of four samples degraded at $T_1 = 25$ °C (yellow). Comparing these results to Fig. 2(a) we find a lower (or even negative) ΔV_{OC} for the ex situ analysis in comparison to the last in situ measurements for the majority of the samples. We attribute this effect to a metastable increase in V_{OC} due to illumination during the LID (see also Section 2) as well as to a slightly different irradiation intensity and spectra in the two set-ups. Furthermore, the ΔV_{OC} shown in Fig. 2 are verified at the respective degradation conditions, impeding the comparison to the ΔV_{OC} verified ex situ at STC. After two weeks of dark storage (DS) we observe a slight enhancement of the V_{OC} for the majority of cells. Regarding the dependency from the illumination intensity during LID we do not observe a clear trend.

For the cells degraded at short circuit conditions we observe a very different degradation behavior of V_{OC} as shown in Fig. 3(b). ΔV_{OC} is negative for all 12 cells degraded at short circuit conditions. The absolute V_{OC} loss for the cells degraded under $G = G_0 = 0\%$ (stars) is small and comparable to the amplitude of V_{OC} change for the case of the cells kept in open circuit during LID (Fig. 3(a)). For the 9 cells degraded at short circuit and light intensities $G > 0\%$ we observe a high loss in V_{OC}. Thereby, the loss is highest for the cells degraded at $T_3 = 70$ °C (brown) with a ΔV_{OC} between −70 and −100 mV. For the cells degraded at low or medium temperature ($T_1 = 25$ °C in yellow and $T_2 = 50$ °C in red) we observe a V_{OC} loss in between −25 and −40 mV absolute. Again regarding differences due to the illumination intensity during LID we do not observe a clear trend. Comparing these results to Fig. 2(b) we find similarly to the OC case a lower (more negative) ΔV_{OC} for the ex situ analysis in comparison to the last in situ measurements for all samples. As before, we attribute this to metastabilities as well as to the difference in the conditions during the measurements. Analogous to the cells degraded at open circuit, for the cells degraded at short circuit we observe a slight enhancement of the V_{OC} for the majority of cells after two weeks of dark storage.

Fig. 4 shows the absolute change in J_{SC} due to LID for all 24 degraded CIGS solar cells. With the exception of one cell (Degradation at $G = G_0$ and $T = T_3$) all cells degraded under short circuit conditions (Fig. 4(b)) show nearly no change in short circuit current density after LID ($-0.1\,\text{mA/cm}^2 < \Delta I_{SC} < 0.15\,\text{mA/cm}^2$). For the cells degraded at open circuit (Fig. 4(a)) we find a slightly reduced short circuit current density after LID (changes up to $-0.65\,\text{mA/cm}^2$). Thereby, there is no clear trend of degradation light intensity and or temperature visible. Note that even the highest absolute change in J_{SC} corresponds to a small relative change of less than 2% (compare with Table 1). After two weeks of DS we observe for the majority of cells a slight enhancement of J_{SC} w.r.t. the STC measurement directly after the LID.

The maximum power point voltage V_{MPP} at STC shows similar changes as V_{OC} at STC for all degraded cells, where cells degraded at short circuit and $T = T_3 = 70$ °C exhibit the highest V_{MPP} loss and all cells degraded at open circuit show only slight changes in V_{MPP} (not shown). For the maximum power point current density J_{MPP} at

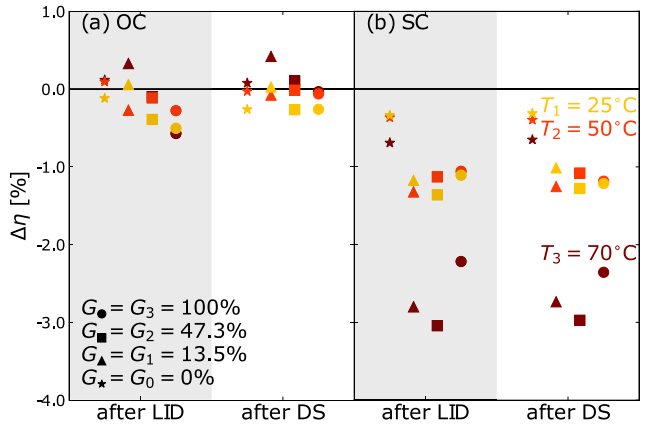

Fig. 5. Absolute change in efficiency $\Delta\eta$ due to LID at (a) open circuit and (b) short circuit conditions. To differ between all degradation conditions we use the same color- and marker scheme used before in Figs. 2–4.

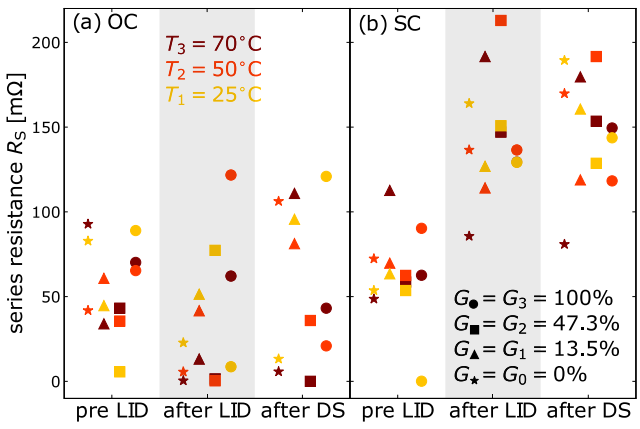

Fig. 6. Series resistance R_S determined from a one diode model fit to JV characteristics measured at STC conditions before and after LID as well as after two weeks of dark storage for the cells kept at (a) open circuit and (b) short circuit conditions during LID. The color indicates the degradation temperatures, i.e. yellow corresponds to $T = T_1 = 25$ °C, red to $T = T_2 = 50$ °C and brown to $T = T_3 = 70$ °C. With the markers we differ for the irradiation levels of $G = G_0 = 0\%$ (stars), $G = G_1 = 13.5\%$ (triangles), $G = G_2 = 47.3\%$ (squares) and $G = G_3 = 100\%$ (circles) during degradation.

STC we observe a slight loss (between −0.02 and −0.76 mA/cm^2) after LID for the cells degraded at open circuit (not shown) and therefore similar absolute changes observed for J_{SC}. For cells degraded at short circuit we also observe only slight changes ($-0.35\,\text{mA/cm}^2 < \Delta J_{MPP} < 0.15\,\text{mA/cm}^2$, not shown), where a loss in J_{MPP} is correlated to the loss in V_{OC} (Fig. 3) and therefore highest for the cells degraded at $T = T_3$.

Regarding the absolute change in efficiency at STC $\Delta\eta$ in Fig. 5 we observe, that all cells degraded at open circuit exhibit small changes due to LID ($-0.5\% < \Delta\eta < 0.5\%$). For the cells degraded at short circuit we observe a loss in STC efficiency of up to −3.1% absolute. Comparing Figs. 3 and 5 we observe, that the loss in efficiency is mainly connected with the loss in V_{OC} respectively V_{MPP}.

5. Discussion

The results presented in Section 4 show that LID appears to be strongly dependent on the conditions CIGS solar cells are degraded at. The performance of CIGS solar cells after 1170 h of LID under open circuit conditions appears to be more or less stable with overall efficiency changes of less then ±0.5% absolute. For LID under short circuit conditions we find an efficiency drop of up to −3.1% absolute caused by a loss in V_{OC} respectively V_{MPP}. This drop in efficiency seems to be more or less independent of the degradation light intensity, while the degradation temperature appears to be crucial for the underlying mechanisms. The cells degraded at low ($T = T_1 = 25$ °C) respectively moderate ($T = T_2 = 50$ °C) temperatures degrade much less then cells degraded at high $T = T_3 = 70$ °C temperature conditions.

By now we only used the SSPs to evaluate changes due to LID. To further investigate the observed V_{OC} drop we use the open source PV-CRAZE library [48]. PV-CRAZE provides a robust fitting algorithm for the one diode model according to Shockley [49]. The current density voltage relation for a p–n junction reads:

$$J(V) = J_{ph} - J_0\left[\exp\left(\frac{V + J(V)R_S A}{nkT/q}\right) - 1\right] - \frac{V + J(V)R_S A}{R_{sh}A}, \quad (1)$$

where I_{ph} represents the photo generated current density, R_S respectively R_{sh} series respectively shunt resistance of the device, n the diode ideality factor, A the cell area, q the elementary charge, k the Boltzmann constant and

$$J_0 = J_{00}\left(\frac{T}{T_0}\right)^3 \exp\left(\frac{-E_g}{nkT}\right) \quad (2)$$

the dark saturation current density. As expected we find a strong correlation of J_{ph} and J_{SC} and therefore only small changes in J_{ph} due to the LID (not shown). Fig. 6 shows the development of R_S for all 24 cells derived from the JV characteristics measured under STC directly before and after LID as well as after 2 weeks of DS. We find a clear trend of increasing series resistance after LID for the cells kept under short circuit conditions (see Fig. 6(b)). For the series resistance of the cells degraded at open circuit conditions we find no clear trend (see Fig. 6(a)). Overall the observed changes and absolute value of the series resistance is small for the whole batch with a maximum of 0.21 Ω. Furthermore, due to the definition of the open circuit voltage ($J(V_{OC}) = 0$) an increased series resistance cannot be the cause for the observed drop in V_{OC}. For the comparison of the shunt resistance before and after LID as well as after dark storage we do not observe a clear trend regarding the degradation conditions (not shown). The shunt resistance varies within the batch of solar cells in a range of 200 to 1000 Ω (outliers only occur to higher resistances) and therefore in a range, which has slight to no negative influence on the solar cells performance.

Fig. 7 shows the determined dark saturation current density J_0 for all cells before, after and after two weeks of dark storage after LID. Contrary to the observed V_{OC} loss in cells degraded at short circuit (see Fig. 3(b)) J_0 tends to increase only slightly for the cells degraded at open circuit (Fig. 7(a)), while a rather constant J_0 is observed for the cells degraded at short circuit (Fig. 7(b)). Beside the dark saturation current density J_0 the diode ideality factor is essential to describe recombination in solar cells according to the one diode model. Fig. 8 shows the determined diode ideality factor for all 24 cells. First of all we observe high ideality factors between 1.85 and 2.3 before LID. After LID the majority of cells degraded at open circuit show an enhanced ideality factor (Fig. 8(a)), while the majority of cells degraded at short circuit exhibit a reduced ideality factor (Fig. 8(b)).

To put the combined effects of the observed changes in J_0 and n into context we define a recombination current density J_x as

$$J_x = J_0 \exp\frac{qV_x}{nkT}, \quad (3)$$

which is the total recombination in the device as a fixed internal voltage V_x (i.e. voltage over the diode without series resistance). Fig. 9 shows the recombination current density J_x at $V_x = 0.7$ V and the from the one diode model determined J_0 and n (Figs. 7 and 8). Note that we choose $V_x = 0.7$ V to show the recombination current close to the initial V_{OC} (the mean V_{OC} across the used batch of CIGS solar cells before LID is 739.5 mV, see Table 1). We observe a strong correlation of J_x with the observed change in V_{OC} and efficiency η (see Figs. 3

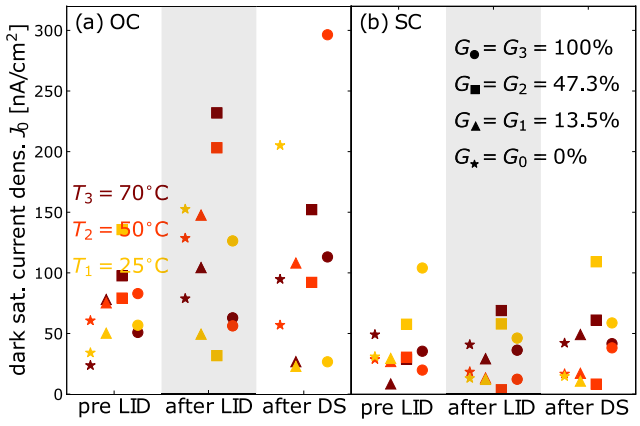

Fig. 7. Dark saturation current density J_0 determined from a one diode model fit to JV characteristics measured at STC conditions before and after LID at (a) open circuit and (b) short circuit conditions as well as after two weeks of dark storage (DS). To differ between all degradation conditions we use the same color- and marker scheme used before in Figs. 2–6.

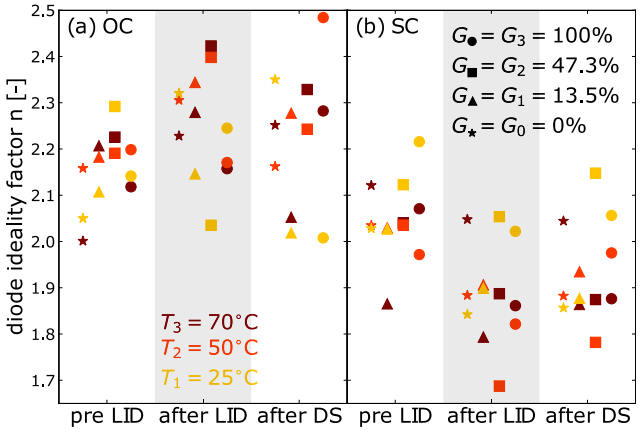

Fig. 8. Diode ideality factor n determined from a one diode model fit to JV characteristics measured at STC conditions before and after LID at (a) open circuit and (b) short circuit conditions as well as after two weeks of dark storage (DS). To differ between all degradation conditions we use the same color- and marker scheme used before in Figs. 2–7.

and 5). We conclude, that LID of CIGS solar cells at short circuit leads to an enhanced recombination and associated open circuit voltage and efficiency loss.

It is interesting to note that the degradation on V_{OC} is associated with a reduction in the ideality factor. This indicates that the increased recombination rate is due to a process with ideality factor 1. This in turn is an indication that additional recombination centers are located in quasi-neutral regions of the device (i.e. not within the depletion region) or are shallow traps [50].[7]

6. Summary and outlook

The presented work describes a detailed study of temperature, bias and intensity dependent light induced degradation of industrially produced encapsulated CIGS solar cells. The results show, that the bias

[7] The derivation in Section 2 of this paper focuses on the activation energy of recombination in *p-i-n* devices. However, the derivation is valid for Shockley–Read–Hall (SRH) recombination in general, and, the paper also discusses the spatial and energetic variation of the ideality factor of SRH recombination.

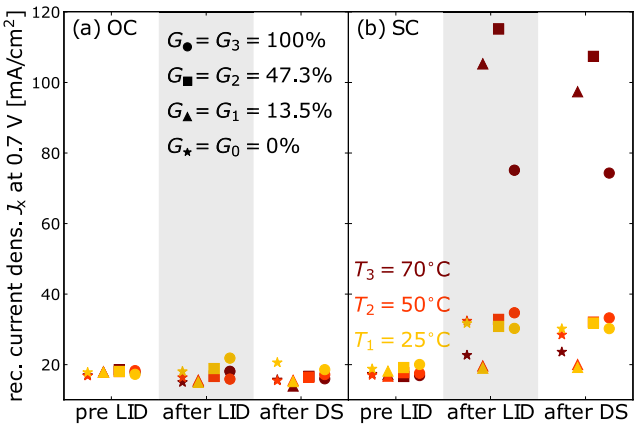

Fig. 9. Recombination current density $J_x = J_0 \exp \frac{qV_x}{nkT}$ at $V_x = 0.7$ V determined from a one diode model fit to JV characteristics measured at STC conditions before and after LID at (a) open circuit and (b) short circuit conditions as well as after two weeks of dark storage (DS). To differ between all degradation conditions we use the same color- and marker scheme used before in Figs. 2–8.

condition is crucial w.r.t. observed performance changes, where cells kept in OC appear to be stable under illumination and cells kept in SC exhibit a performance drop of up to 3% absolute (efficiency at STC) within 1170 h of light exposure. The performance drop is shown to be dependent on the temperature condition during LID, while being more or less independent on the irradiation intensity. Furthermore, it is observed that the overall recombination rate increases and, at the same time, the ideality factor is reduced. This indicates that the increased recombination rate is due to a process with ideality factor 1, consistent with recombination centers located in quasi-neutral regions of the device. Due to the observed big discrepancy between performance stability at OC and SC, and the fact that CIGS modules are operated somewhere between these extreme bias conditions (optimally at MPP), future work should concentrate on filling this gap, aiming to depict a bias condition closer to real operation scenarios.

CRediT authorship contribution statement

T.S. Vaas: Writing – review & editing, Writing – original draft, Visualization, Software, Methodology, Investigation, Formal analysis, Data curation, Conceptualization. **B.E. Pieters:** Writing – review & editing, Supervision, Project administration, Conceptualization. **D. Roosen-Melsen:** Writing – review & editing, Resources. **M. van den Nieuwenhof:** Resources. **A. Kingma:** Resources. **M. Theelen:** Writing – review & editing, Resources. **C. Zahren:** Writing – review & editing, Investigation, Data curation. **A. Gerber:** Writing – review & editing, Supervision, Project administration, Conceptualization. **U. Rau:** Writing – review & editing, Supervision, Resources, Project administration.

Declaration of competing interest

The authors declare the following financial interests/personal relationships which may be considered as potential competing interests: This work has been partially funded by the Federal Ministry of Education under the Helmholtz LLEC Project, and the Ministry of Culture and Science of the State of North Rhine-Westphalia under the grant B1610.01.17. We kindly thank Niklas Bongartz for the assistance during the characterization of the solar cells. If there are other authors, they declare that they have no known competing financial interests or personal relationships that could have appeared to influence the work reported in this paper.

Data availability

Data will be made available on request.

Acknowledgments

This work has been partially funded by the Federal Ministry of Education under the Helmholtz LLEC Project, and the Ministry of Culture and Science of the State of North Rhine-Westphalia under the grant B1610.01.17. We kindly thank Niklas Bongartz for the assistance during the characterization of the solar cells.

Appendix

See Fig. 10.

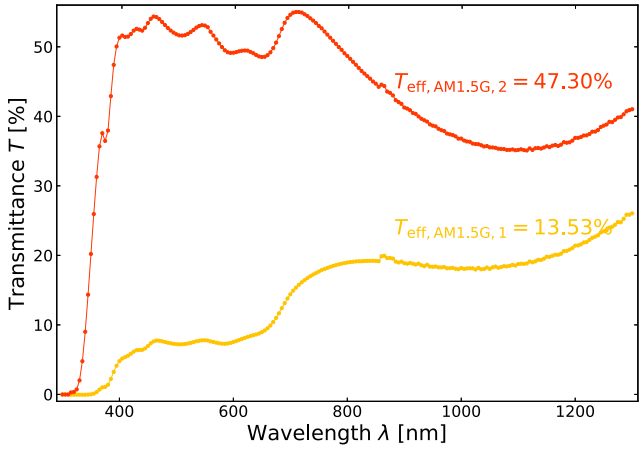

Fig. 10. Transmittance of the used ND filters in the wavelength range between 300 and 1300 nm. Using the AM1.5G photon flux we find an effective Transmittance of $T_{\text{eff,AM1.5G,1}} = 13.53\%$ and $T_{\text{eff,AM1.5G,2}} = 47.30\%$.

References

[1] NREL, Best research-cell efficiency chart, 2023, URL https://www.nrel.gov/pv/cell-efficiency.html.

[2] M. Theelen, F. Daume, Stability of Cu(In,Ga)Se_2 solar cells: A literature review, Sol. Energy 133 (2016) 586–627.

[3] J. Kettle, M. Aghaei, S. Ahmad, A. Fairbrother, S. Irvine, J.J. Jacobsson, S. Kazim, V. Kazukauskas, D. Lamb, K. Lobato, et al., Review of technology specific degradation in crystalline silicon, cadmium telluride, copper indium gallium selenide, dye sensitised, organic and perovskite solar cells in photovoltaic modules: Understanding how reliability improvements in mature technologies can enhance emerging technologies, Prog. Photovolt., Res. Appl. 30 (12) (2022) 1365–1392.

[4] M. Schweiger, J. Bonilla, W. Herrmann, A. Gerber, U. Rau, Performance stability of photovoltaic modules in different climates, Prog. Photovoltaics: Res. Appl. 25 (12) (2017) 968–981.

[5] G. Makrides, B. Zinsser, M. Schubert, G.E. Georghiou, Performance loss rate of twelve photovoltaic technologies under field conditions using statistical techniques, Sol. Energy 103 (2014) 28–42.

[6] M.N. Ruberto, A. Rothwarf, Time-dependent open-circuit voltage in $CuInSe_2$/CdS solar cells: Theory and experiment, J. Appl. Phys. 61 (9) (1987) 4662–4669.

[7] D. Willett, S. Kuriyagawa, The effects of sweep rate, voltage bias and light soaking on the measurement of CIS-based solar cell characteristics, in: Conference Record of the Twenty Third IEEE Photovoltaic Specialists Conference-1993 (Cat. No. 93CH3283-9), IEEE, 1993, pp. 495–500.

[8] R. Sasala, J. Sites, Time dependent voltage in $CuInSe_2$ and CdTe solar cells, in: Conference Record of the Twenty Third IEEE Photovoltaic Specialists Conference-1993 (Cat. No. 93CH3283-9), IEEE, 1993, pp. 543–548.

[9] F. Engelhardt, M. Schmidt, T. Meyer, O. Seifert, J. Parisi, U. Rau, Metastable electrical transport in Cu(In,Ga)Se_2 thin films and ZnO/CdS/Cu(In,Ga)Se_2 heterostructures, Phys. Lett. A 245 (5) (1998) 489–493.

[10] M. Igalson, A. Kubiaczyk, P. Zabierowski, Deep centers and fill factor losses in the CIGS devices, MRS Online Proc. Libr. (OPL) 668 (2001) H9–2.

[11] C. Walkons, M. Jahandardoost, T.M. Friedlmeier, W. Hempel, S. Paetel, M. Nardone, B. Ursprung, E.S. Barnard, K.E. Kweon, V. Lordi, et al., Behavior of Na and RbF-treated CdS/cu(in,ga)se_2 solar cells with stress testing under heat, light, and junction bias, Phys. Status Solidi (RRL)–Rapid Res. Lett. 15 (2) (2021) 2000530.

[12] M. Sodhi, L. Banaszek, C. Magee, M. Rivero-Hudec, Economic lifetimes of solar panels, Procedia CIRP 105 (2022) 782–787.

[13] P.-O. Westin, P. Neretnieks, M. Edoff, Damp heat degradation of CIGS-based PV modules, in: 21st European Photovoltaic Solar Energy Conference, 2006, pp. 2470–2473.

[14] D.-W. Lee, O.-Y. Kwon, J.-K. Song, C.-H. Park, K.-E. Park, S.-M. Nam, Y.-N. Kim, Effects of ZnO:Al films on CIGS PV modules degraded under accelerated damp heat, Sol. Energy Mater. Sol. Cells 105 (2012) 15–20.

[15] D.-w. Lee, W.-j. Cho, C.-i. Jang, J.-k. Song, C.-h. Park, K.-e. Park, J.-s. Ryu, H. Lee, Y.-n. Kim, Damp heat and thermal cycling-induced degradation mechanism of AZO and CIGS films in Cu(In,Ga)Se_2 photovoltaic modules, Curr. Appl. Phys. 15 (3) (2015) 285–291.

[16] M. Theelen, R. Hendrikx, N. Barreau, H. Steijvers, A. Böttger, The effect of damp heat-illumination exposure on CIGS solar cells: A combined XRD and electrical characterization study, Sol. Energy Mater. Sol. Cells 157 (2016) 943–952.

[17] M. Theelen, K. Beyeler, H. Steijvers, N. Barreau, Stability of CIGS solar cells under illumination with damp heat and dry heat: A comparison, Sol. Energy Mater. Sol. Cells 166 (2017) 262–268.

[18] J. Malmström, J. Wennerberg, L. Stolt, A study of the influence of the Ga content on the long-term stability of Cu(In,Ga)Se_2 thin film solar cells, Thin Solid Films 431 (2003) 436–442.

[19] M. Theelen, K. Polman, M. Tomassini, N. Barreau, H. Steijvers, J. van Berkum, Z. Vroon, M. Zeman, Influence of deposition pressure and selenisation on damp heat degradation of the Cu(In,Ga)Se_2 back contact molybdenum, Surf. Coat. Technol. 252 (2014) 157–167.

[20] M. Theelen, S. Harel, M. Verschuren, M. Tomassini, A. Hovestad, N. Barreau, J. van Berkum, Z. Vroon, M. Zeman, Influence of Mo/$MoSe_2$ microstructure on the damp heat stability of the Cu(In,Ga)Se_2 back contact molybdenum, Thin Solid Films 612 (2016) 381–392.

[21] V. Fjällström, P.M.P. Salomé, A. Hultqvist, M. Edoff, T. Jarmar, B.G. Aitken, K. Zhang, K. Fuller, C.K. Williams, Potential-induced degradation of $CuIn_{1-x}Ga_x Se_2$ thin film solar cells, IEEE J. Photovolt. 3 (3) (2013) 1090–1094, http://dx.doi.org/10.1109/JPHOTOV.2013.2253833.

[22] P. Yilmaz, J. de Wild, R. Aninat, T. Weber, B. Vermang, J. Schmitz, M. Theelen, In-depth analysis of potential-induced degradation in a commercial CIGS PV module, Prog. Photovolt., Res. Appl. (2023).

[23] S. Lee, S. Bae, S.J. Park, J. Gwak, J. Yun, Y. Kang, D. Kim, Y.-J. Eo, H.-S. Lee, Characterization of potential-induced degradation and recovery in CIGS solar cells, Energies 14 (15) (2021) 4628.

[24] S.P. Harvey, H. Guthrey, C.P. Muzzillo, G. Teeter, L. Mansfield, P. Hacke, S. Johnston, M. Al-Jassim, Investigating PID shunting in polycrystalline CIGS devices via multi-scale, multi-technique characterization, IEEE J. Photovolt. 9 (2) (2019) 559–564.

[25] S. Yamaguchi, S. Jonai, K. Hara, H. Komaki, Y. Shimizu-Kamikawa, H. Shibata, S. Niki, Y. Kawakami, A. Masuda, Potential-induced degradation of Cu(In,Ga)Se_2 photovoltaic modules, Japan. J. Appl. Phys. 54 (8S1) (2015) 08KC13.

[26] O. Salomon, W. Hempel, O. Kiowski, E. Lotter, W. Witte, A. Ferati, A. Schneikart, G. Kaune, R. Schäffler, M. Becker, et al., Influence of molybdenum back contact on the PID effect for Cu(In,Ga)Se_2 solar cells, Coatings 9 (12) (2019) 794.

[27] C.P. Muzzillo, K. Terwilliger, P. Hacke, H.R. Moutinho, M.R. Young, S. Glynn, B. Stevens, I.L. Repins, L.M. Mansfield, Potential-induced degradation of Cu(In,Ga)Se2 can occur by shunting the front i-ZnO and by damaging the p-n junction, Sol. Energy 232 (2022) 298–303.

[28] V. Fjällström, P. Szaniawski, B. Vermang, P.M.P. Salomé, F. Rostvall, U. Zimmermann, M. Edoff, Recovery after potential-induced degradation of $CuIn_1 - x Ga_x Se_2$ solar cells with CdS and Zn(O,S) buffer layers, IEEE J. Photovolt. 5 (2) (2015) 664–669, http://dx.doi.org/10.1109/JPHOTOV.2014.2384839.

[29] U. Rau, M. Schmitt, J. Parisi, W. Riedl, F. Karg, Persistent photoconductivity in Cu(In,Ga)Se_2 heterojunctions and thin films prepared by sequential deposition, Appl. Phys. Lett. 73 (2) (1998) 223–225.

[30] T. Meyer, M. Schmidt, F. Engelhardt, J. Parisi, U. Rau, A model for the open circuit voltage relaxation in Cu(In,Ga)Se_2 heterojunction solar cells, Eur. Phys. J. Appl. Phys. 8 (1) (1999) 43–52.

[31] J. Heath, J. Cohen, W. Shafarman, Distinguishing metastable changes in bulk CIGS defect densities from interface effects, Thin Solid Films 431 (2003) 426–430.

[32] I. Eisgruber, J. Granata, J. Sites, J. Hou, J. Kessler, Blue-photon modification of nonstandard diode barrier in cuinse$_2$ solar cells, Sol. Energy Mater. Sol. Cells 53 (3–4) (1998) 367–377.

[33] M. Igalson, H. Schock, The metastable changes of the trap spectra of cuinse$_2$-based photovoltaic devices, J. Appl. Phys. 80 (10) (1996) 5765–5769.

[34] V. Nádaždy, M. Yakushev, E. Djebbar, A. Hill, R. Tomlinson, Switching of deep levels in $CuInSe_2$ due to electric field-induced Cu ion migration, J. Appl. Phys. 84 (8) (1998) 4322–4326.

[35] M. Igalson, M. Cwil, M. Edoff, Metastabilities in the electrical characteristics of CIGS devices: Experimental results vs theoretical predictions, Thin Solid Films 515 (15) (2007) 6142–6146.
[36] I. Repins, S. Glynn, T.J. Silverman, R. Garris, K. Bowers, B. Stevens, L. Mansfield, Large metastability in cu(in,ga)se_2 devices: The importance of buffer properties, Prog. Photovolt., Res. Appl. 27 (9) (2019) 749–759.
[37] I. Repins, S. Glynn, K. Bowers, B. Stevens, C.L. Perkins, L. Mansfield, Using hole injection layers for decreased metastability and higher performance in cu(in,ga)se_2 devices, Sol. Energy Mater. Sol. Cells 215 (2020) 110597.
[38] S. Lany, A. Zunger, Light-and bias-induced metastabilities in Cu(In,Ga)Se_2 based solar cells caused by the (V_{Se}-V_{Cu}) vacancy complex, J. Appl. Phys. 100 (11) (2006).
[39] M. Maciaszek, P. Zabierowski, On the magnitude of the persistent photoconductivity (PPC) effect in CIGS layers with and without sodium, in: 2015 IEEE 42nd Photovoltaic Specialist Conference, PVSC, IEEE, 2015, pp. 1–3.
[40] K. Macielak, M. Maciaszek, M. Igalson, P. Zabierowski, N. Barreau, Persistent photoconductivity in polycrystalline Cu(In,Ga)Se_2 thin films: Experiment versus theoretical predictions, IEEE J. Photovolt. 5 (4) (2015) 1206–1211.
[41] F. Obereigner, N. Barreau, W. Witte, R. Scheer, Open-circuit and doping transients of Cu(In,Ga)Se_2 solar cells with varying Ga content, J. Appl. Phys. 117 (5) (2015).
[42] J.-F. Guillemoles, L. Kronik, D. Cahen, U. Rau, A. Jasenek, H.-W. Schock, Stability issues of Cu(In,Ga)Se_2-based solar cells, J. Phys. Chem. B 104 (20) (2000) 4849–4862.
[43] S. Ishizuka, N. Taguchi, P.J. Fons, Similarities and critical differences in heavy alkali-metal rubidium and cesium effects on chalcopyrite Cu(In,Ga)Se_2 thin-film solar cells, J. Phys. Chem. C 123 (29) (2019) 17757–17764.
[44] M. Gostein, L. Dunn, Light soaking effects on photovoltaic modules: Overview and literature review, in: 2011 37th IEEE Photovoltaic Specialists Conference, IEEE, 2011, pp. 003126–003131.
[45] A. Kanevce, S. Paetel, D. Hariskos, T.M. Friedlmeier, Impact of rbf-PDT on Cu(In,Ga)Se_2 solar cells with cds and Zn(o,s) buffer layers, EPJ Photovoltaics 11 (2020) 8.
[46] C. Zhao, S. Yu, W. Tang, X. Yuan, H. Zhou, T. Qi, X. Zheng, D. Ning, M. Ma, J. Zhu, et al., Advances in CIGS thin film solar cells with emphasis on the alkali element post-deposition treatment, Mater. Rep.: Energy (2023) 100214.
[47] M.H.-T. Corp, Flexible Solar Cell Datasheet, Brochure, 2022, URL https://miasole.com/wp-content/uploads/2022/07/SolarCell_10x_Datasheet_B.pdf. (Accessed 5 November 2023).
[48] B. Pieters, PV-CRAZE, 2023, https://github.com/PVCRAZE/.
[49] W. Shockley, The theory of p-n junctions in semiconductors and p-n junction transistors, Bell Syst. Tech. J. 28 (3) (1949) 435–489.
[50] B. Pieters, H. Stiebig, M. Zeman, R. Van Swaaij, Determination of the mobility gap of intrinsic μc-Si: H in pin solar cells, J. Appl. Phys. 105 (4) (2009).